

In Situ X-ray Absorption Spectroscopy Study of $\text{Si}_{1-x}\text{Ge}_x\text{O}_2$ Dissolution and Germanium Aqueous Speciation under Hydrothermal Conditions

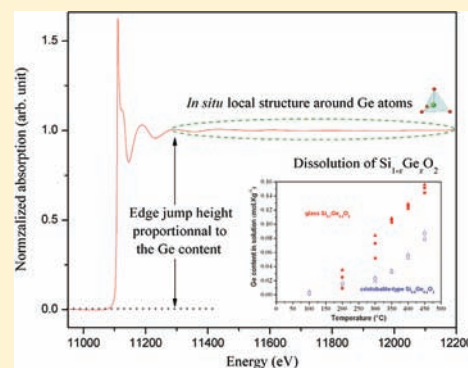
V. Ranieri,^{*,†} J. Haines,[†] O. Cambon,^{*,†} C. Levelut,[‡] R. Le Parc,[‡] M. Cambon,[†] and J.-L. Hazemann[§]

[†]Institut Charles Gerhardt de Montpellier, C2M, UMR5253, CNRS-UM2-ENSCM-UM1, Université Montpellier 2, cc1504, Place E. Bataillon, F-34095 Montpellier Cedex 5, France

[‡]Laboratoire Charles Coulomb, UMR 5221, CNRS-UM2, Université Montpellier 2, cc026, Place E. Bataillon, F-34095 Montpellier Cedex 5, France

[§]Département MCMF, Institut Néel, CNRS-Grenoble, 25 avenue des Martyrs, B.P. 166, 38042 Grenoble Cedex 9, France

ABSTRACT: The dissolution of $\text{Si}_{1-x}\text{Ge}_x\text{O}_2$ solid solutions under hydrothermal conditions was studied by in situ X-ray absorption spectroscopy. Experiments were performed at the Ge K-edge using a high-pressure cell mounted on the FAME beamline of the European Synchrotron Radiation Facility. Spectra in both transmission and fluorescence mode were collected in isobaric conditions (100 and 150 MPa) up to 475 °C. The local atomic structure around the Ge atom was investigated as a function of the temperature and in pure water and sodium hydroxide solutions. In pure water, the solubility of the cristobalite-type $\text{Si}_{0.8}\text{Ge}_{0.2}\text{O}_2$ increases with the temperature and the Ge atom is in 4-fold coordination. In a sodium hydroxide aqueous solution, a complex between Ge and Na atoms forms and gives rise to precipitation of sodium germanates. Under these conditions, the Ge content in the solution decreases with increasing temperature. These results show that a sodium hydroxide aqueous solution, usually used for quartz crystal growth, is not suitable for Ge-containing crystals. The dissolution kinetics and phase transformation of the solid solution were studied as a function of the atomic fraction of Ge. Ge-rich solid solutions dissolve and transform to stable phases faster than Ge-poorer composition, giving rise to important variations of the Ge content in solution.



INTRODUCTION

In the field of piezoelectric materials, quartz is still widely used. However, its physical properties are too limited for emerging applications. Structure–property relationships linking the thermal stability of the α -quartz-type phase and the physical properties (dielectric, piezoelectric, etc.) to the structural distortion with respect to the β -quartz structure type have been developed for α -quartz homeotypes.^{1–9} Germanium substitution in the α -quartz lattice is believed to be a promising way to increase the distortion and thereby improve these properties.

The growth of α -quartz-type $\text{Si}_{1-x}\text{Ge}_x\text{O}_2$ single crystals by the hydrothermal vertical temperature gradient method is controlled by the dissolution kinetics and transport of the species.¹⁰ Because of the large difference of the dissolution kinetics between GeO_2 ¹¹ and SiO_2 ,¹² solid solutions have been prepared by thermal treatment and used as a starting material.¹⁰ The knowledge of the dissolution behavior of the starting material under hydrothermal conditions is a crucial parameter in a crystal growth experiment. The concentrations of solvated species are usually determined by the mass loss method. However, further information such as the dissolution kinetics and local atomic structure can be obtained by in situ X-ray absorption spectroscopy (XAS). XAS measurements can be

performed on the BM30B FAME beamline of the European Synchrotron Radiation Facility (ESRF) using an X-ray optical high-pressure cell. This setup is very efficient in order to determine at the same time the solubility of a solid phase and the local structure around a given element.^{11,13,14} However, it was reported in the literature that intense X-ray light can modify aqueous solution properties creating radicals and also modify the oxidation state of hydrated metals such as gold or copper.^{15–18} This sensitivity to irradiation may involve a change of the dissolution kinetics. Previous work on the system GeO_2 – H_2O did not show any problems related to beam damage.¹¹ In the present study, we used the high-pressure cell to measure the dissolution kinetics of $\text{Si}_{1-x}\text{Ge}_x\text{O}_2$ ($0.2 < x < 0.5$) solid phases with different structure types in a sodium hydroxide (NaOH) aqueous solution and water (H_2O). Indeed, the phase diagram of the SiO_2 – GeO_2 system indicates that α -quartz-type solid solutions exist with a maximum of 31 atom % GeO_2 at about 700 °C and 70 MPa under hydrothermal conditions,¹⁹ but the single crystals obtained in 1 M NaOH (conditions of industrial synthetic quartz growth) do not contain more than 0.6 atom % Ge. A reason mentioned is the formation of a

Received: August 25, 2011

Published: December 16, 2011



sodium germanate^{20–23} phase, which traps Ge atoms during the dissolution process, but until now, no in situ measurements had been used to study the evolution of the Ge concentration in solution under hydrothermal conditions. The present XAS study was performed to better understand the hydrothermal process and to provide useful information for developing the crystal growth process.

EXPERIMENTAL SECTION

Sample Preparation. $\text{Si}_{1-x}\text{Ge}_x\text{O}_2$ solid solutions were prepared by thermal treatment from commercial α -quartz powder (Fluka) and α -quartz-type GeO_2 (Stanford Materials). The stoichiometric mixture was homogenized for 4 h and melted at 1685 °C for 24 h. The samples were then cooled in order to obtain either the cristobalite type or the glass forms. The different phases were identified by powder X-ray diffraction measurements performed on a PANalytical X'Pert diffractometer equipped with an X'celerator detector using Ni-filtered $\text{Cu K}\alpha$ radiation. The chemical composition was measured using a CAMECA SX100 electron probe microanalysis instrument equipped with five wavelength-dispersive X-ray spectrometers.

In Situ X-ray Absorption Fine Structure (XAFS) Measurement. XAFS spectra were collected in both transmission and fluorescence mode at the Ge K-edge (11.103 eV) over the energy range 10.900–11.800 eV at the bending magnet-based BM30b beamline of the ESRF (Grenoble, France). The storage ring was operated at 6 GeV with a 200 mA current. The beam energy was selected using a Si(220) double-crystal monochromator. The beam size on the sample was focused to 300 μm horizontally and 130 μm vertically, thus keeping a high X-ray photon flux ($\sim 10^{12}$ photon/s).

Samples and solutions were placed in a high-pressure cell developed at the Institut Néel (Grenoble, France).²⁴ The apparatus consists of a glassy carbon cell inserted into a superhigh-tension steel vessel. The vessel has a water-cooling jacket and three beryllium windows for the X-ray beam. The cell contains a vertically oriented outer glassy carbon tube (internal diameter of about 5 mm) with walls of about 0.2 mm thickness and two carbon coaxial inner rods delimiting the sample space below and above. The sample and solution were placed in the gap between these two inner rods. The temperature in the sample space is maintained within ± 0.2 °C by molybdenum heating resistances and Pt–Pt/Rh thermocouples connected to a Eurotherm temperature regulator. The internal temperature of the cell was calibrated by calculating the density of H_2O based on XAS measurements and comparing it with values from the National Institute of Standards and Technology (NIST).²⁵ The autoclave was pressurized by high-purity-grade helium gas with a low X-ray absorption cross section.

Several experiments were performed under the same thermodynamic conditions in order to study the influence of three parameters (composition of the aqueous solution, composition of the solid solution, and structure type) on the $\text{Si}_{1-x}\text{Ge}_x\text{O}_2$ dissolution process. The experiments consisted of measuring the transmission and fluorescence XAFS spectra of the solution under isobaric conditions (100 and 150 MPa) from 20 °C up to 475 °C. A preliminary experiment on the dissolution of cristobalite-type $\text{Si}_{0.8}\text{Ge}_{0.2}\text{O}_2$ was performed by using the weight loss method in a 100 cm^3 autoclave with the aim of evaluating the amount of material dissolved.

The transmission X-ray absorption signal was used to determine the Ge aqueous concentration. Indeed, the absorption jump over the Ge edge is directly related to the amount of the absorbing element in solution. The solvent contribution to the absorption does not vary significantly over the Ge K-edge, and the amplitude of the absorption edge height at given T and P can be written as

$$\Delta\mu = \Delta\sigma_{\text{Ge}}xM_{\text{Ge}}m_{\text{Ge}}d_{\text{fluid}}$$

where $\Delta\sigma_{\text{Ge}}$ is the change of the total absorption cross section of Ge over its K edge (cm^2/g), x is the optical path length inside the cell (cm), M_{Ge} is the atomic weight (0.072 59 kg/mol), m_{Ge} is the molal Ge aqueous concentration (mol/kg of solution), and d_{fluid} is the density of the aqueous solution (g/cm^3)

at given T and P . The absorption cross sections of Ge before and after its edge were taken from the Elam²⁶ tables. Data analysis was performed using the software *Athena* and *Artemis* from the *Horae* package.²⁷ The pre-edge and post-edge parts of the XAFS spectra are fitted with spline curves, and the differences between the two lines are taken as the value of $\Delta\mu$. The following fitting procedure was used: normalization of the spectra to the absorption edge height, extraction of the EXAFS oscillations $\chi(k)$ with evaluation of the baseline, and fitting of the distance to the neighboring shells (R) and EXAFS Debye–Waller factor (noted as σ^2 and referring to the mean-square relative displacement to which this technique is sensitive). The parameter ΔE_0 , which accounts for the error in determining the edge energy, was also fitted. The amplitude factor (SO^2) was fixed to 1. All fits were performed in the R space.

RESULTS AND DISCUSSION

1. XAS Study of $\text{Si}_{1-x}\text{Ge}_x\text{O}_2$ Dissolution. Spectra in both the fluorescence and transmission mode were recorded at the Ge K-edge.

The evolution of the transmission spectra and absorption edge during the dissolution of $\text{Si}_{0.8}\text{Ge}_{0.2}\text{O}_2$ in a 0.5 M NaOH aqueous solution and pure H_2O is presented in Figure 1a,b.

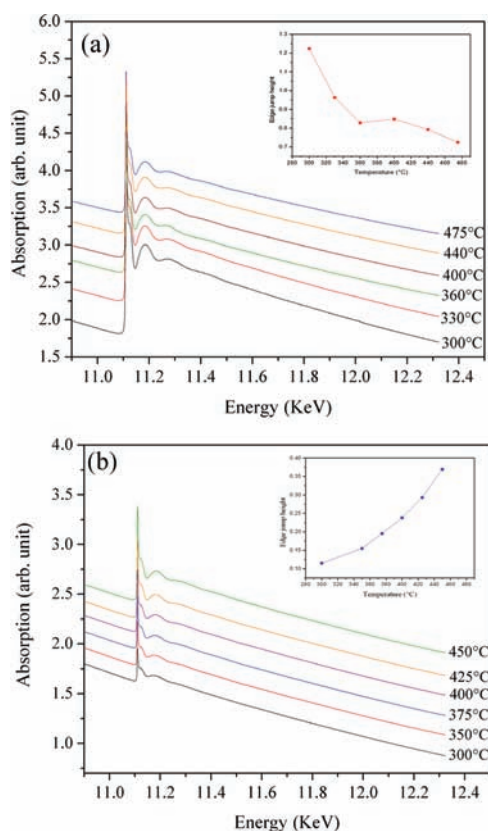


Figure 1. XAFS transmission spectra of a 0.5 M NaOH aqueous solution (a) and H_2O (b) at 150 MPa during the dissolution of cristobalite-type $\text{Si}_{0.8}\text{Ge}_{0.2}\text{O}_2$ as a function of the temperature. The evolution of the edge jump height as a function of the temperature is presented in the inset.

The edge jump in the case of a NaOH aqueous solution is important and decreases rapidly above 300 °C, whereas it remains small in H_2O even at 450 °C, showing that the dissolution process is more efficient in an alkaline solution.

i. 0.5 M NaOH. The Ge concentration during the dissolution experiment in a 0.5 M NaOH aqueous solution presents a maximum value at 300 °C (Figure 2). A dramatic

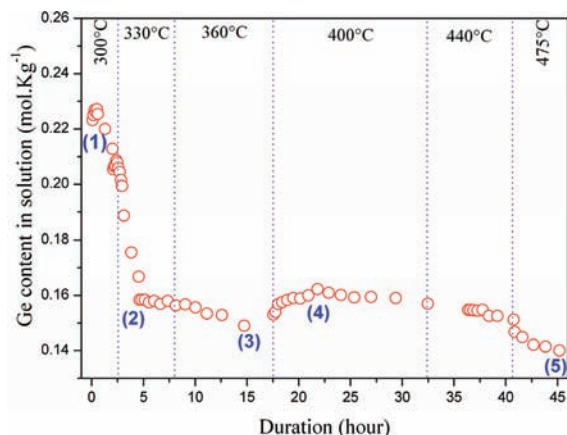


Figure 2. Evolution of the Ge content in a NaOH aqueous solution as a function of the time and temperature during the dissolution of cristobalite-type $\text{Si}_{0.8}\text{Ge}_{0.2}\text{O}_2$.

decrease occurs during the first 4 h, and then the amount of Ge in solution stabilizes around 0.16 mol/kg.

Powder X-ray diffraction analysis of the recovered sample shows that the entire sample transforms to two different phases (Figure 3): a $\text{Si}_{1-x}\text{Ge}_x\text{O}_2$ ($x \leq 0.05$) phase with the α -quartz-type structure and a second phase $\text{Na}_4\text{Ge}_9\text{O}_{20}$.

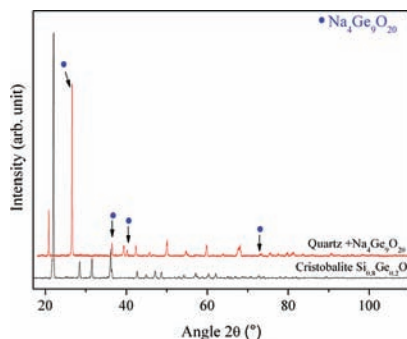


Figure 3. X-ray diffraction patterns of the material before and after the dissolution experiment in aqueous 0.5 M NaOH.

Thus, three different processes are in competition: (i) the dissolution of cristobalite-type $\text{Si}_{0.8}\text{Ge}_{0.2}\text{O}_2$, (ii) the formation and precipitation of $\text{Na}_4\text{Ge}_9\text{O}_{20}$, and (iii) the transformation to stable phases (cristobalite to α -quartz). The influence of each process is displayed in Figure 2: (1) Up to 300 °C, the dissolution is predominant and the Ge concentration in solution is high (0.23 mol/kg), (1 and 2) above this concentration, the $\text{Na}_4\text{Ge}_9\text{O}_{20}$ complex forms and precipitates involving an important decrease of the Ge content in solution. Between (2) and (3), the influence of the phase transformation appears. At constant temperature (360 °C), the Ge content decreases. The solution is supersaturated with respect to the solid phase and the excess of species in solution precipitates. Over 5 h (3 and 4), the change in the temperature enhances the dissolution, and from point (4) to (5), the influence of the phase transformation becomes stronger and the concentration of Ge decreases again. Point (5) can be interpreted as the end of the phase transformation. The solution

is supersaturated with respect to the new stable phases, and thus the species in excess precipitate until the equilibrium state between solid phases and solution has been reached.

ii. H₂O. The evolution of Ge in H_2O was investigated starting from three different samples: cristobalite-type $\text{Si}_{0.8}\text{Ge}_{0.2}\text{O}_2$ and two glasses with 30 and 50 atom % Ge.

The dissolution process in H_2O is quite different. For the cristobalite-type $\text{Si}_{0.8}\text{Ge}_{0.2}\text{O}_2$ and the glass with 30 atom % Ge, the evolution of the Ge content in solution increases continuously with temperature, showing the absence of precipitation of any Ge-containing compound (Figure 4). The glass is

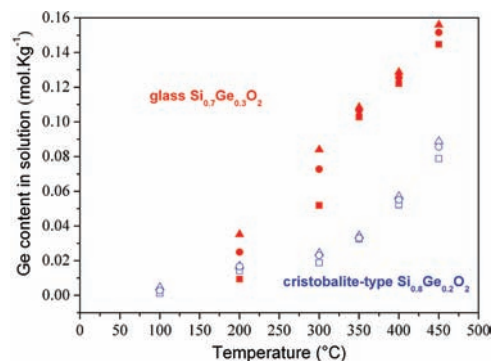


Figure 4. Evolution of the Ge content in pure H_2O as a function of the temperature and time. Open and solid symbols represent respectively the values obtained during the dissolution of cristobalite-type $\text{Si}_{0.8}\text{Ge}_{0.2}\text{O}_2$ (blue) and $\text{Si}_{0.7}\text{Ge}_{0.3}\text{O}_2$ glass (red) after 10 min (squares), 40 min (circles), and 80 min (triangles) of stabilization.

more quickly dissolved than the cristobalite phase. Even if the dissolution kinetics are more rapid in the NaOH aqueous solvent, the Ge content in solution reaches a similar value (~ 0.16 mol/kg) at 450 °C upon dissolution of the glass phase, while the value remains lower for cristobalite dissolution. The X-ray diffraction data for the recovered material show that the cristobalite-type sample is not fully transformed to the stable α -quartz-type phase (Figure 5). The dissolution and phase

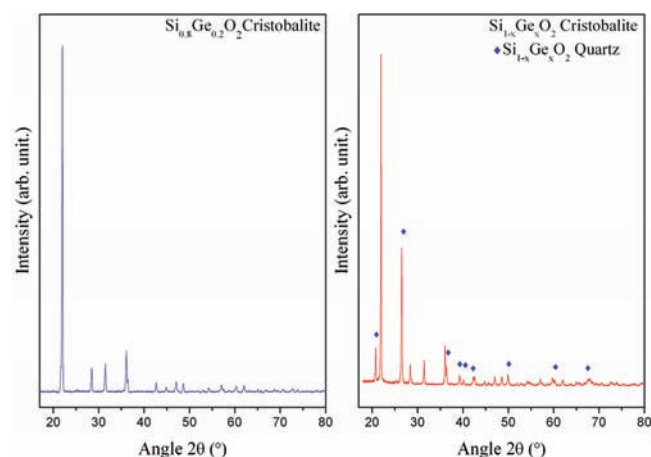


Figure 5. X-ray diffraction patterns of the material before and after the dissolution experiments in pure H_2O .

transformation kinetics of cristobalite-type $\text{Si}_{0.8}\text{Ge}_{0.2}\text{O}_2$ are slower in H_2O than in the NaOH aqueous solution, and over the total duration of the experiment (16 h), the dissolution process remains predominant.

The concentration of Ge in solution increases faster as a function of the temperature and time during the dissolution of a glass with 30 atom % Ge. Above 300 °C, the equilibrium state between the solid and solution is reached in 10 min. Over the 16 h of the experiment, the glass is not fully transformed to stable phases and the dissolution process is still predominant. Under the same conditions, the evolution of the Ge content in H₂O during the dissolution of a glass with 50 atom % Ge is very different (Figure 6). Starting from low temperatures, the Ge

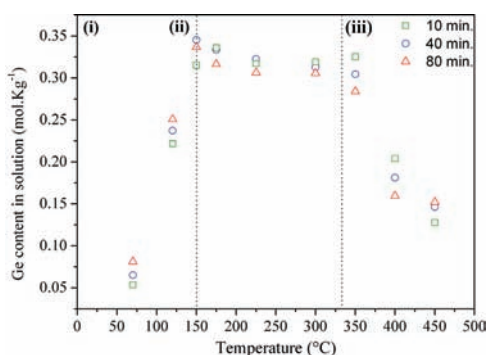


Figure 6. Evolution of the Ge concentration during the dissolution of a Si_{0.5}Ge_{0.5}O₂ glass in H₂O as a function of the temperature and time.

content increases quickly, but above 150 °C, the process is reversed: the concentration decreases slightly with temperature and time. Above 350 °C, a dramatic decrease occurs within 10 min and continues with time and temperature.

This profile can be explained by a series of phase transformations. Indeed, X-ray diffraction on the recovered solid phase shows that the glass completely transforms to rutile-type GeO₂ and α -quartz-type ($x \leq 0.03$) stable phases during the experiment (Figure 7). Several equilibrium states between

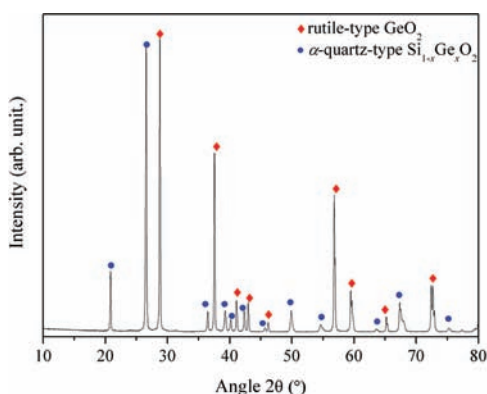


Figure 7. X-ray diffraction pattern of the material after the dissolution experiment in pure H₂O.

the solid phases and solution can be assigned to each of the three regions defined in Figure 6. In the first region (i), the glass dissolves. Because of the high Ge content, the dissolution process is rapid and thus the Ge content in solution is high and dissolution is predominant. In the second region (ii), the solution is in a metastable equilibrium with three different solid phases: glass, α -quartz-type Si_{1-x}Ge_xO₂, and rutile-type GeO₂. The competition between the dissolution, phase transformation, and recrystallization leads to a relatively stable Ge concentration up to 350 °C. With respect to the first region,

precipitation dominates with respect to the dissolution and the Ge content decreases with time. The recrystallization process becomes more important. In the last region (iii), the phase transformation is complete; the solution is supersaturated with respect to the stable phases: rutile-type GeO₂ and α -quartz-type Si_{1-x}Ge_xO₂. The crystallization process dominates, and the Ge content in solution decreases up to 450 °C. At this temperature, the dissolution occurs during the first 40 min and then the Ge content in solution stabilizes around 0.15 mol/kg.

2. Local Structure around Ge Atoms in Solution. k^2 -weighted EXAFS fluorescence spectra and an example of fitted reverse Fourier transformation are presented in Figure 8. The

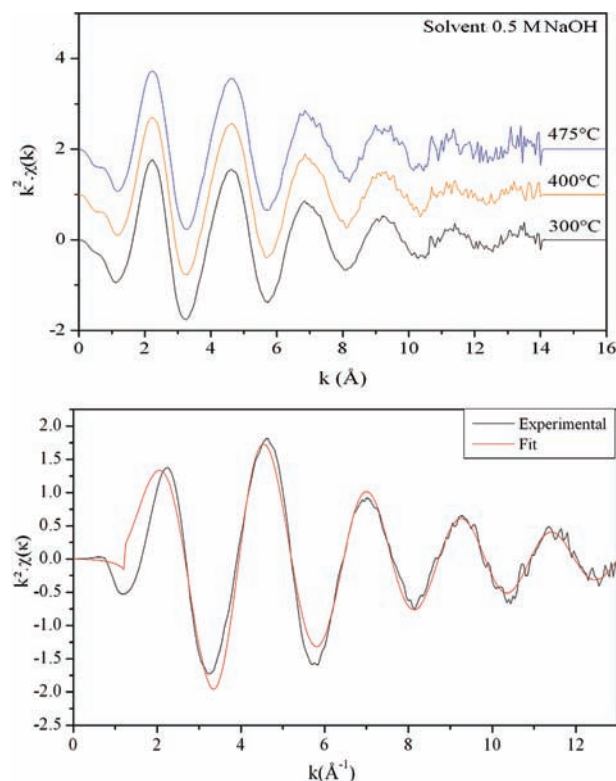


Figure 8. Normalized k^2 -weighted EXAFS fluorescence spectra as a function of the temperature (top) and examples of fitted reverse Fourier transformation (bottom).

XAFS oscillations show very similar shapes and no significant changes in the pressure–temperature (P – T) range studied. The Fourier transformation magnitude of the EXAFS spectra (Figure 9) shows a first-shell contribution from GeO₄ tetrahedra. The second contribution observed is due to multiple scattering (MS) within the GeO₄ tetrahedra and not to a Ge–Ge bond.¹¹ The refinement of the oscillations exhibits a first-shell contribution from 4 ± 0.5 O atoms at 1.76 ± 0.02 Å, which is in good agreement with the literature.^{7,10} No significant evolution of the structure is observed in the P – T range studied (Tables 1–3). The Debye–Waller factor (σ^2) is almost stable, denoting that the strongly covalent Ge–O bond is not very sensitive to temperature. The Debye–Waller factor σ^2 is slightly higher in a NaOH aqueous solution, suggesting a distortion of the GeO₄ tetrahedron (Table 1). This is consistent with previous studies, which show that aqueous Ge species correspond to the neutral Ge(OH)₄ complex at pH < 9

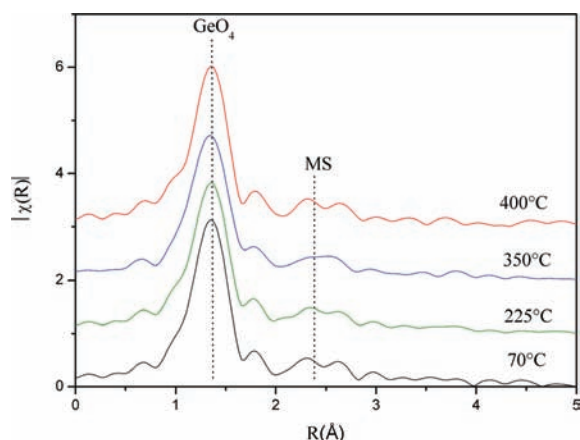


Figure 9. Fourier transformation magnitudes (not corrected for the phase shift) of normalized k^2 -weighted EXAFS spectra of H_2O during the dissolution of the $\text{Si}_{0.5}\text{Ge}_{0.5}\text{O}_2$ glass in H_2O at 100 MPa.

Table 1. Fitting Parameters and Agreement Factor Obtained from Analysis of the Ge K-Edge EXAFS Spectra in a 0.5 M NaOH Aqueous Solution during the Dissolution of the $\text{Si}_{0.8}\text{Ge}_{0.2}\text{O}_2$ Cristobalite Type as a Function of the Temperature at 150 MPa

T (°C)	k range (Å^{-1})	r_0 (Å)	N_0	σ^2 (10^{-3}Å^2)	ΔE (eV)	R factor
300	2.0–12.3	1.76(1)	4.2(2)	4.2(4)	6.3(4)	0.0001
330	2.0–12.3	1.76(1)	3.9(2)	3.9(6)	5.2(6)	0.0003
400	2.0–12.3	1.76(1)	3.9(2)	4.1(7)	5.2(8)	0.0005
440	2.0–12.3	1.76(2)	3.9(2)	4.0(4)	5.3(5)	0.0002
475	2.0–12.3	1.76(2)	4.1(2)	4.4(3)	5.9(5)	0.0002

Table 2. Fitting Parameters and Agreement Factor Obtained from Analysis of the Ge K-Edge EXAFS Spectra in Pure H_2O (18 MΩ) during the Dissolution of the $\text{Si}_{0.8}\text{Ge}_{0.2}\text{O}_2$ Cristobalite Type as a Function of the Temperature at 150 MPa

T (°C)	k range (Å^{-1})	r_0 (Å)	N_0	σ^2 (10^{-3}Å^2)	ΔE (eV)	R factor
300	2.0–12	1.76(2)	4.0(2)	3.5(6)	6.1(6)	0.0010
375	2.0–12	1.76(2)	3.8(2)	3.4(6)	5.7(5)	0.0009
400	2.0–12	1.76(1)	3.6(2)	3.3(5)	5.8(5)	0.0008
425	2.0–12	1.76(1)	3.6(2)	3.6(6)	5.9(6)	0.0008
450	2.0–11.2	1.75(2)	3.5(2)	3.2(7)	5.6(6)	0.0007

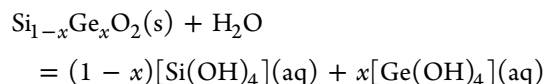
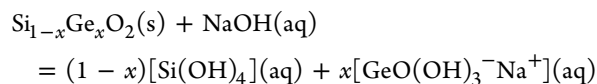
Table 3. Fitting Parameters and Agreement Factor Obtained from Analysis of the Ge K-Edge EXAFS Spectra in Pure H_2O (18 MΩ) during the Dissolution of a $\text{Si}_{0.5}\text{Ge}_{0.5}\text{O}_2$ Glass as a Function of the Temperature at 100 MPa

T (°C)	k range (Å^{-1})	r_0 (Å)	N_0	σ^2 (10^{-3}Å^2)	ΔE (eV)	R factor
70	2.0–12.9	1.75(1)	4.4(4)	1.8(8)	4(1)	0.0009
225	2.0–12.9	1.75(2)	4.1(3)	2.1(8)	4(1)	0.0009
350	2.0–12.9	1.76(2)	4.4(4)	3.1(9)	4(1)	0.0007
450	2.0–12.9	1.75(2)	4.1(2)	2.1(6)	4(1)	0.0005

and are dominated by the negative $\text{GeO}(\text{OH})_3^-$ species at higher pH.^{28,29}

The general reaction of the dissolution of $\text{Si}_{1-x}\text{Ge}_x\text{O}_2$ depends only on the nature of the aqueous solution. In a

NaOH aqueous solution and in H_2O , the reaction can be respectively described as follows:



CONCLUSION

The dissolution of $\text{Si}_{1-x}\text{Ge}_x\text{O}_2$ ($0.2 < x < 0.5$) solid solutions was studied by in situ XAS using a high-pressure cell. In situ XAS measurements provide key information about the dissolution kinetics and the local structure around Ge atoms as a function of the solvent and solid solution composition. As expected, the dissolution and phase transformation kinetics of cristobalite-type $\text{Si}_{0.8}\text{Ge}_{0.2}\text{O}_2$ are higher in a NaOH aqueous solution. However, above the concentration of 0.23 mol/kg, the Ge content decreased strongly as a function of time. This decrease is linked to the formation of relatively insoluble sodium germanates $\text{Na}_4\text{Ge}_9\text{O}_{20}$. In pure H_2O , these phenomena are slower, but over our time-scale experiment, the Ge concentration increases continuously with the temperature. The NaOH aqueous solution is clearly not suitable for the hydrothermal crystal growth in our P – T range. The dissolution is more efficient, but the formation of sodium germanates limits the amount of Ge in solution and thus in the crystal grown. The dissolution and phase transformation kinetics increase with the Ge content in the solid phase. The tetrahedral structures $\text{Ge}(\text{OH})_4$ and $\text{GeO}(\text{OH})_3^-$ are found to be very stable over the P – T range investigated. XAS is a very powerful and unique technique to investigate the evolution of the concentration and the local structure around a given element during the dissolution process under hydrothermal conditions.

AUTHOR INFORMATION

Corresponding Author

*E-mail: vranieri@esrf.fr (V.R.), ocambon@lpmc.univ-montp2.fr (O.C.).

ACKNOWLEDGMENTS

We are grateful to the CRG scientific committee for providing synchrotron beam time. We thank the FAME team for welcoming us and for their help during the experiment. We also thank the French Ministry of Defense for financial support (Contract 05 34 051) and the three anonymous reviewers for their useful comments.

REFERENCES

- Philippot, E.; Goiffon, A.; Ibanez, A.; Pintard, M. *J. Solid State Chem.* **1994**, *110*, 356.
- Philippot, E.; Palmier, D.; Pintard, M.; Goiffon, A. *J. Solid State Chem.* **1996**, *123*, 1–13.
- Philippot, E.; Armand, P.; Yot, P.; Cambon, O.; Goiffon, A.; Mcintyre, J.; Bordet, P. *J. Solid State Chem.* **1999**, *146*, 114–123.
- Haines, J.; Château, C.; Léger, J.-M.; Marchand, R. *Ann. Chim. Sci. Mater.* **2001**, *26*, 209–216.
- Haines, J.; Cambon, O.; Hull, S. Z. *Kristallogr.* **2003**, *218* (3), 193–200.
- Cambon, O.; Yot, P.; Ruhl, S.; Haines, J.; Philippot, E. *Solid State Sci.* **2003**, *5*, 469.

- (7) Haines, J.; Cambon, O.; Philippot, E.; Chapon, L.; Hull, S. J. *Solid State Chem.* **2002**, *166*, 434.
- (8) Cambon, O.; Haines, J.; Frayssé, G.; Detaint, J.; Capelle, B.; Van der Lee, A. *J. Appl. Phys.* **2005**, *97*.
- (9) Ranieri, V.; Bourgogne, D.; Darracq, S.; Cambon, M.; Haines, J.; Cambon, O.; Le Parc, R.; Levelut, C.; Largeteau, A.; Demazeau, G. *Phys. Rev. B* **2009**, *79*, 224304.
- (10) Ranieri, V.; Darracq, S.; Cambon, M.; Haines, J.; Cambon, O.; Largeteau, A.; Demazeau, G. *Inorg. Chem.* **2011**, DOI: 10.1021/ic200354p.
- (11) Pokrovski, G.; Roux, J. S.; Hazemann, J.-L.; Testemale, D. *Chem. Geol.* **2005**, *217* (1–2), 127–145.
- (12) Manning, C. E. *Geochim. Cosmochim. Acta* **1994**, *58*, 4831–4839.
- (13) Pokrovski, G.; Borisova, A.; Roux, J.; Hazemann, J.-L.; Petdang, A.; Tella, M.; Testemale, D. *Geochim. Cosmochim. Acta* **2006**, *70*, 4196–4214.
- (14) Testemale, D.; Dufaud, F.; Martinez, I.; Bénézech, P.; Hazemann, J.-L.; Schott, J.; Guyot, F. *Chem. Geol.* **2009**, *259*, 8–16.
- (15) Mesu, J. G.; van der Eerden, A. M. J.; de Groot, F. M. F.; Weckhuysen, B. M. J. *Phys. Chem. B* **2005**, *109*, 4042–4047.
- (16) James-Smith, J.; Cauzid, J.; Testemale, D.; Liu, W.; Hazemann, J.-L.; Proux, O.; Etschmann, B.; Philippot, P.; Banks, D.; Williams, P.; Brugger, J. *Am. Mineral.* **2010**, *95*, 921–932.
- (17) Brugger, J.; Etschmann, B.; Liu, W.; Testemale, D.; Hazemann, J.-L.; van Beek, W.; Proux, O. *Geochim. Cosmochim. Acta* **2007**, *71*, 4920–4941.
- (18) Pokrovski, G. S.; Tagirov, B. R.; Schott, J.; Bazarkina, E. F.; Hazemann, J. L.; Proux, O. *Chem. Geol.* **2009**, *259* (1–2), 17–29.
- (19) Miller, W. S.; Datchell, F.; Shafer, E. C.; Roy, R. *Am. Mineral.* **1963**, *48*, 1024.
- (20) Roy, R.; Theokritoff, S. *J. Cryst. Growth* **1972**, *12*, 69–72.
- (21) Passaret, M.; Toudic, Y.; Regreny, A.; Aumont, R.; Bayon, J. F. *J. Cryst. Growth* **1972**, *13/14*, 524–529.
- (22) Balitsky, D. V.; Balitsky, V. S.; Pushcharovsky, D. Yu.; Bondarenko, G. V.; Kosenko, A. V. *J. Cryst. Growth* **1997**, *180*, 212–219.
- (23) Balitsky, D. V.; Balitsky, V. S.; Pisarevsky, Y. V.; Philippot, E.; Silvestrova, O. Y.; Puscharovsky, D. Y. *Ann. Chim. Sci. Matér.* **2001**, *26* (1), 183–192.
- (24) Testemale, D.; Argoud, R.; Geaymond, O.; Hazemann, J.-L. *Rev. Sci. Instrum.* **2005**, *76*, 043905–043909.
- (25) <http://webbook.nist.gov/chemistry/>.
- (26) Elam, W. T.; Ravel, B.; Sieber, J. R. *Radiat. Phys. Chem.* **2002**, *63*, 121–128.
- (27) Ravel, B.; Newville, M. *J. Synchrotron Radiat.* **2005**, *12*, 537–541.
- (28) Baes, C. F., Jr.; Mesmer, R. E. *The Hydrolysis of Cations*; Wiley: New York, 1976.
- (29) Pokrovski, G. S.; Schott, J. *Geochim. Cosmochim. Acta* **1998**, *62*, 3413–342.